CMOS-level-voltage Substrate-removed Thin-film Lithium Niobate Modulator

Mengyue Xu, Shengqian Gao, Heyun Tan, Xinlun Cai
State Key Laboratory of Optoelectronic Materials and Technologies and School of Electronics and Information Technology, Guangzhou 510275, China.
caixlun5@mail.sysu.edu.cn

Abstract: We demonstrate an O-band substrate-removed thin-film lithium niobate modulator with a low microwave loss of 0.24 dB cm^{-1} GHz$^{-1/2}$. The device features a 1-V half-wave voltage and 1.4 dB EO response roll-off at 50 GHz. © 2022 The Author(s)

1. Introduction

Lithium niobate on insulator (LNOI) platform is promising for high-speed modulation [1-3], due to its strong Pockels effect, femtosecond timescale electro-optic (EO) response, and low optical loss. The microwave propagation loss is a detrimental factor in decreasing the bandwidth of the traveling-wave modulator, especially for a long modulation length which is necessary for a low drive voltage. The two main types of microwave loss (α_m) are dielectric loss and conductor loss [4]. Dielectric loss is closely related to the substrate material, and conductor loss is highly dependent on electrode design. Thin-film LN modulator with capacitively loaded traveling-wave electrode (CL-TWE) had demonstrated ultra-low microwave losses (0.26 dB cm^{-1} GHz$^{-1/2}$) on quartz substrate [1]. The air can offer lower permittivity and intrinsic loss ($\tan\delta_D$) than quartz, resulting in a lower dielectric loss. Air gaps underlying TWE can be formed by isotropic etching silicon substrate [5-6]. Besides, the silicon substrate is compatible with microelectronics and is low-cost.

In this paper, we demonstrate a substrate-removed LN Mach-Zehnder modulator (MZM) with CL-TWE on the LN-on-silicon platform. The microwave loss is greatly reduced to 0.24 dB cm^{-1} GHz$^{-1/2}$ due to substrate removal. We achieve perfect velocity matching by optimizing the CL-TWE and controlling the depth of the air gap. The fabricated device features a half-wave voltage (V_π) of 1V and an electro-optic response with a 1.4 dB roll-off at 50 GHz at the O-band.

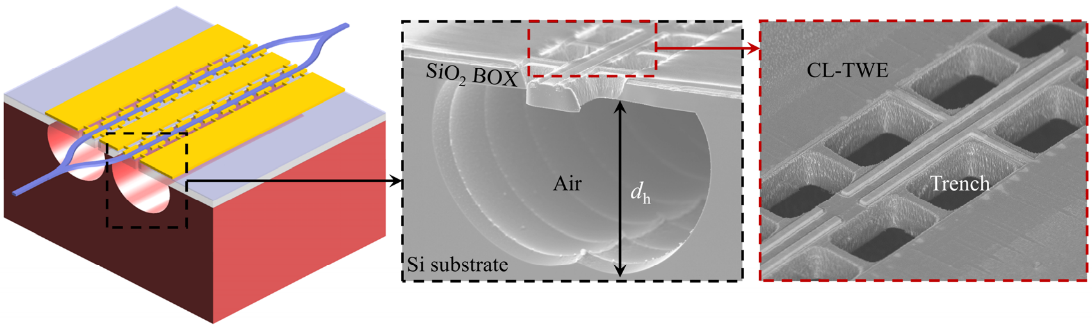

Fig.1. Schematic diagram and SEM images of the silicon-removed LNOI-based modulator.

2. Substrate-removed MZM design and fabrication

The proposal substrate-removed device structure is depicted in Fig. 1. The device was fabricated on an LN-SiO_2-silicon wafer with a 3-μm SiO_2 layer and the high-resistivity silicon substrate for negligible substrate leakage loss. The MZM adopts optimized CL-TWE in ground-signal-ground (GSG) configuration, where the two etched LN waveguides lie in the gaps of the T-rails of ground and signal electrodes. The 900-nm-thick Au electrodes are deposited and patterned with the lift-off process. Then, we patterned and dry-etched the LN film and SiO_2 around the T-rails of the CL-TWE to form the deep air trenches down to the silicon substrate. Finally, we removed the silicon substrate underlying the electrodes by the dry etching process. The etching depth is controllable by adjusting the etching time.

Because silicon has a relatively large tanδ_D of 0.043 [7], the silicon substrate needs to be removed in areas where the microwave electric field is concentrated to minimize dielectric loss. We adopt a depth of air gap (d_h) of 17 µm and the mostly electric field is propagation in the air instead of silicon (Fig. 2. (a)). Meanwhile, the value of d_h is inversely proportional to the microwave group indices. Perfect matching between the depth of air gap can be achieved when d_h is around 17 µm.

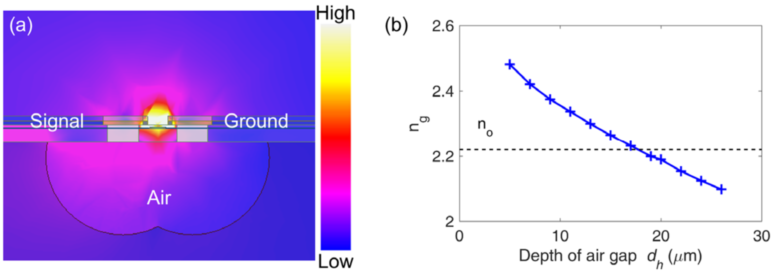

Fig. 2. (a) Simulated microwave electric field distribution. (b) Calculated microwave mode indices (50 GHz) as a function of air gap depth.

3. Experimental results

The microwave performance of CL-TWE determines the bandwidth and transmission performance of the modulator to a large extent. We measured the small-signal response using a 67-GHz vector network analyzer (VNA) with all external probes and coaxial lines de-embedded. As shown in Fig.3 (a), the fabricated 20-mm CL-TWE has low electrical reflection below -24 dB in the frequency range from 0.1 GHz to 67 GHz, showing good impedance matching. The velocity between microwave and optical waves is well matched in the test frequency range (Fig. 3(b)), indicating the depth of the air gap is close to our prediction.

We extract the RF loss from the measure EE response of the CL-TWE with silicon removal and the regular TWE. As shown in Fig. 3(a-b), the α_m of the CL-TWE adopted in this work (0.24 dB cm^{-1} GHz$^{-1/2}$) is significantly lower than that in regular TWE (0.62 dB cm^{-1} GHz$^{-1/2}$). The α_m of the CL-TWE and frequency show a square root dependence, from which it can be inferred that the air gap minimizes the dielectric loss and the conductor loss dominates [4].

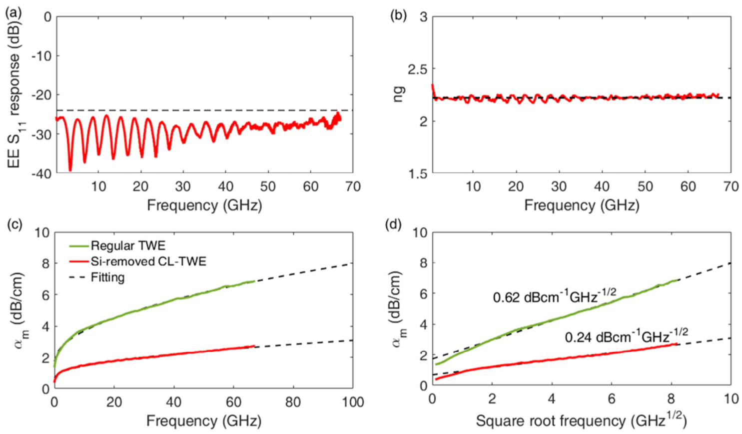

Fig. 3. (a) Measured electrical reflection, (b) measured microwave mode index, and (c-d) measured microwave losses (solid lines) of a 20-mm silicon-removed thin-film LN MZM.

We characterize the low-frequency V_π and the EO response of the 20-mm-long modulator at the wavelength of 1310 nm. As shown in Fig. 4. (a), the measured V_π is 1 V, corresponding to the modulation efficiency of 2 Vcm. The EO S_{21} magnitude indicates a 1.4 dB roll-off at 50 GHz (Fig. 4. (b)). The 3-dB bandwidth is well beyond the measurement limit from our 50-GHz photodetector (Finisar XPDV2320). In Fig. 4. (b), we also extrapolate the expected 3-dB EO bandwidth performance based on the measured α_m to beyond 100 GHz.

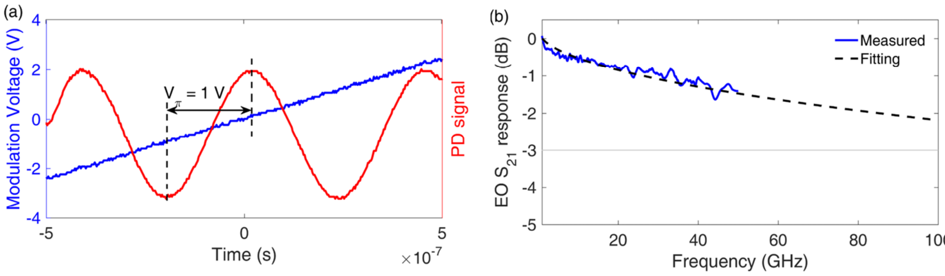

Fig. 4. (a) Measured half-wave voltage and (b) measured (blue solid line) and simulated (black dash line) EO S_{21} response of a 20-mm silicon-removed thin-film LN MZM.

4. Conclusion

We demonstrate a 20-mm-long substrate-removed modulator on the LN-on-silicon platform. The microwave loss is significantly reduced by removing silicon and using optimized CL-TWEs. The fabricated device features a COMS-compatible V_π (1 V), a 1.4 dB EO response roll-off at 50 GHz, and the 3-dB bandwidth is predicted beyond 100 GHz. The silicon removal process used in this work is compatible with fabricating thermal isolation trenches and cantilever structures, which shows the great potential for monolithic integration with power-efficient thermal-optic phase shifters [5] and low-loss cantilever edge couplers [8].

5. References

[1]. P. Kharel, C. Reimer, K. Luke, L. He, and M. Zhang, "Breaking voltage–bandwidth limits in integrated lithium niobate modulators using micro-structured electrodes," Optica **8**, 357-363 (2021).

[2]. M. Xu, et al., "High-performance coherent optical modulators based on thin-film lithium niobate platform," Nature Communications 11, 3911 (2020).

[3]. M. Xu, et al., "Integrated thin film lithium niobate Fabry–Perot modulator," Chin. Opt. Lett. 19, 060003 (2021).

[4] J. Zhang, S. Alexandrou and T. Y. Hsiang, "Attenuation characteristics of coplanar waveguides at subterahertz frequencies," *IEEE Transactions on Microwave Theory and Techniques*, 53, 3281-3287 (2005)

[5] M. F. Li, L. Wang, X. Li, X. Xiao, and S. H. Yu, "Silicon intensity Mach-Zehnder modulator for single lane 100 Gb/s applications," Photonics Res. **6**, 109-116 (2018).

[6]. S. Gao, et al., "Power-Efficient Thermal Optical Tunable Grating Coupler Based on Silicon Photonic Platform," IEEE Photonics Technol. Lett. **31**, 537-540 (2019).

[7]. R. Yang, C. Hung, Y. Su, M. Weng, and H. Wu, "Loss characteristics of silicon substrate with different resistivities," Microwave and Optical Technology Letters **48**, 1773-1776 (2006).

[8]. S. Gao, L. Chen, and X. Cai, "Cantilever Edge Coupler for Lithium Niobate On Insulator Platform," in Conference on Lasers and Electro-Optics (Optical Society of America, San Jose, California, 2021), p. JW1A.61.